Sectional anatomic and magnetic resonance imaging features of coelomic structures of loggerhead sea turtles

Ana Luisa S. Valente, DVM, MSc; Rafaela Cuenca, DVM, PhD; Maria Angeles Zamora, DM; Maria Luz Parga, DVM, MSc; Santiago Lavin, DVM, PhD; Ferrán Alegre, DVM; and Ignasi Marco, DVM, PhD

Objective—To compare cross-sectional anatomic specimens with images obtained via magnetic resonance imaging (MRI) of the coelomic structures of loggerhead sea turtles (*Caretta caretta*).

Animals—5 clinically normal live turtles and 5 dead turtles.

Procedures—MRI was used to produce T1- and T2-weighted images of the turtles, which were compared with gross anatomic sections of 3 of the 5 dead turtles. The other 2 dead turtles received injection with latex and were dissected to provide additional cardiovascular anatomic data.

Results—The general view on the 3 oriented planes provided good understanding of cross-sectional anatomic features. Likewise, major anatomic structures such as the esophagus, stomach, lungs, intestine (duodenum and colon), liver, gallbladder, spleen, kidneys, urinary bladder, heart, bronchi, and vessels could be clearly imaged. It was not possible to recognize the ureters or reproductive tract.

Conclusions and Clinical Relevance—By providing reference information for clinical use, MRI may be valuable for detailed assessment of the internal anatomic structures of loggerhead sea turtles. Drawbacks exist in association with anesthesia and the cost and availability of MRI, but the technique does provide excellent images of most internal organs. Information concerning structures such as the pancreas, ureters, intestinal segments (jejunum and ileum), and the reproductive tract is limited because of inconsistent visualization. (*Am J Vet Res* 2006;67:1347–1353)

Magnetic resonance imaging is a sophisticated computerized imaging technique used as a clinical diagnostic tool in human medicine since 1971.[1] Compared with other diagnostic imaging tools, MRI has advantages and disadvantages. Magnetic resonance imaging does not use ionizing radiation and is not dangerous to patients or technical personnel.[2] It is a powerful technique for obtaining images of soft tissues in various planes without repositioning of the animal,[3] and it allows visualization of blood vessels without the use of contrast medium.[4] However, more time is required for data analysis when MRI is used, compared with other techniques, and sedation or anesthesia is usually needed. Ferromagnetic objects such as microchips, projectiles, or fishing hooks can cause tissue damage and artifact spots on the image because the static magnetic field and spatial gradient field induce torque and translational forces on an object, which can be displaced or heated.[5] The use of MRI is expensive, compared with other imaging techniques, but its use in wildlife is justified in endangered species because of the amount of diagnostic information that can be gathered in a short period of time and with little risk to the animal.[6-8]

Abbreviation

MRI	Magnetic resonance imaging

Because chelonians have internal viscera entirely covered by osseous structures (carapace and plastron bones), the use of MRI to visualize and evaluate the coelomic structures has several advantages over other conventional techniques that use radiographs, including a representation of detailed cross-sectional anatomic features without distraction from superimposed structures, variations in gray scale formats, enhanced contrast resolution, and computer reconstruction of multiplane images.[9] However, its true potential will only be realized when sufficient clinicians have used the technique on enough turtles to provide accurate interpretation of the resulting images.[10]

Some authors have reported the MRI appearance of the internal structures in other species of chelonians such as the spur-thighed tortoise (*Testudo graeca*), Aldabra giant tortoise (*Dipsochelys elephantine*), Hermann's tortoise (*Testudo hermani*), central Asian tortoise (*Testudo horsfieldii*), leopard tortoise (*Geochelone pardalis pardalis*), *Kinixys* spp, and the red-eared slider terrapin (*Trachemys scripta elegans*).[9-12] To the authors' knowledge, the literature contains only 1 article that includes a description of gross cross-sectional anatomic features correlated with the use of MRI to detect internal tumors in green turtles (*Chelonia mydas*) with cutaneous fibropapillomatosis,[13] in which the authors describe the normal MRI appearance of this species on the basis of 1 healthy turtle and 3 dead turtles.

The loggerhead sea turtle is an endangered species[14] in the Mediterranean Sea mainly because of high mortality rates caused by fishing activity.[15] As a result, this species is also the most commonly seen in

Received October 25, 2005.
Accepted March 1, 2006.
From the Servei d'Ecopatologia de Fauna Salvatge, Facultat de Veterinària, Universitat Autònoma de Barcelona, 08193 Bellaterra, Barcelona, Spain (Valente, Cuenca, Lavin, Marco); the Diagnosis Médica, Córcega 345, 08037 Barcelona, Spain (Zamora); and the Centre de Recuperació d`Turtles Marins, Camí Ral 239, 08330 Premià de Mar, Barcelona, Spain (Parga, Alegre).
The authors thank Dr. Francisco Reina, Isabel Delgado Calvarro, and Angeles Lafuente for technical support.
Address correspondence to Dr. Valente.

rescue centers on the northwestern Mediterranean coast.[16] Most of those turtles have internal damage from hooks, traumatic injuries, or digestive disorders caused by ingestion of garbage.[16] In most cases, complementary diagnostic imaging methods are necessary to establish a diagnosis.

The purpose of the study reported here was to compare cross-sectional anatomic specimens with images obtained via MRI of the coelomic structures of loggerhead sea turtles.

Materials and Methods

Magnetic resonance imaging was performed on 5 live juvenile loggerhead sea turtles, 4 dead juvenile turtles, and 1 dead subadult turtle. Dead turtles were imaged only to correlate the images with corresponding frozen sections to permit description of sectional anatomic features. Description of the MRI findings in clinically normal turtles was based on the 5 healthy turtles. Sex of the turtles could not be identified because they were sexually immature and were classified as juvenile or subadult according to carapace length.[17] The turtles had a minimum straight carapace length[18] of 29.5 to 49.8 cm and were accidentally caught in pelagic longline sets and fishing nets along the northwestern Mediterranean coast (40°31' to 42°26 N' and 0°32' to 3°10' E) of Spain. For purposes of the present study, only those turtles in which the hook was superficially attached in or near the mouth and easily removed through the oral cavity were included. Live turtles were temporarily housed in the rehabilitation facilities of the Rescue Centre for Marine Turtles, Premiá de Mar, Barcelona, Spain, and were fed mainly sardines. Only turtles in good health, as determined on the basis of results of physical, radiographic, and hematologic examinations, were scanned. Dead turtles were kept frozen until the MRI procedure and were thawed 24 to 48 hours before the MRI procedure, depending on size.

The MRI was performed by use of a 1.5-Tesla superconducting magnet.[a] The imaging protocol consisted of sagittal, transverse, and dorsal spin-echo T1-weighted images (600 to 920/15/2; TR/TE/NEX) and fast spin-echo T2-weighted images (4,050 to 10,000/100/2; TR/TE/NEX), with 4- to 6.6-mm slice thickness without slice interval and a 288 × 192/320 × 224 matrix. Depending on the turtle's size, the sequence variables, mainly the TR and TE, had to be changed. No contrast medium was used.

An initial attempt was made to restrain the head and flippers of the turtles by means of a large self-adhesive band; however, it became necessary to immobilize turtles via IV injection in the dorsal cervical sinus with a combination of ketamine[b] (15 mg/kg) and diazepam[c] (0.5 mg/kg). Prior to the scan, heart rate was checked with a mini-Doppler instrument and the turtles were carefully kept wet. Images were obtained beginning at 180 to 300 seconds after the turtles were adequately sedated.

After the MRI images were obtained, 3 of the 5 scanned dead turtles were placed in individual right-angled polystyrene boxes filled with tap water for the anatomic cross-sectioning study. The boxes with the cadavers were frozen at –80°C for at least 24 hours before anatomic sectioning. Each of the 3 cadavers was sectioned in an oriented plane (sagittal, dorsal, and transverse) to approximate the MRI sections. Serial parallel sections from 18 to 20 mm thick were obtained by use of an electric bone saw. The anatomic sections were thicker than those of the MRI to maintain integrity and position of the anatomic structures in the slices for consultation during the study. It was expected to fit 4 or 5 MRI sections to each anatomic section, considering loss of material from the saw. Slices were immediately washed with 80% ethanol to eliminate frost buildup and remove debris and were then separated by grids. After labeling, the frozen slices were immersed for 30 minutes in neutral-buffered 10% formalin solution for thawing. A digital high-resolution, 2,560 × 1,920- pixel camera[d] and daylight was used to record the image of the fresh surface. Further image processing such as rotation, scaling, cutting, filtering, and corrections for contrast, brightness and color were performed with software.[e] In 2 other dead turtles, latex was injected through the jugular vein and the dorsal aorta. Large heart vessels and renal vasculature were dissected for additional morphologic data. The anatomic terminology applied was that of the *Nomina Anatomica Veterinaria*. Specific terminology for sea turtles[19] was also applied. To map the organs in the coelomic cavity in relation to the turtle's exterior, a digital grid was composed that was superimposed virtually on each MRI dorsal image, with initial adjustment of the anterior and posterior lines of the grid to the cranial and caudal tips of the carapace. For each turtle, the grid was adjusted to carapace size and the quadrants were automatically and proportionally adjusted (**Figure 1**).

Results

In live and dead turtles, better tissue differentiation, and, by extension, easier identification of morphologic structures and organs, was achieved via examination in T2-weighted images. In general, organ contours were not so well defined in the images taken in T1-weighted sequence.

Anatomic structures seen on T2-weighted images of the cadaver specimens matched with structures identified in the corresponding anatomic sections (**Figures 2 and 3**). Compared with the live turtles, the vessels and some parenchymatous organs, such as the liver and the kidney, of the dead specimens had hyperintense signals in T2-weighted images.

In the T1- and T2-weighted images of live and dead turtles, some areas of the carapace and plastron had a different kind of signal (Figures 2 and 4). Three layers could be visualized in the transverse T2-weighted sections of the carapace: a hypointense external layer; a central, slightly hyperintense layer; and a thinner, internal hypointense layer. The inner portion of the carapace was lined by a hyperintense layer that corresponded to the coelomic membrane and fluid. Areas of carapace with an absence of signal in T2-weighted scans were observed in the fontanelles (the nonossified intercostal space in the distal third of the ribs[19]). For the plastron, the connective tissue could be identified in T1-weighted images and only the bones could be visualized in T2-weighted images.

The esophagus was seen as a tubular structure joining the stomach dorsally from the first to the second central quadrant (**Figures 1, 2, and 4–8**) of the coelomic cavity. The esophageal lumen and its conical keratinized papillae were well visualized in transverse and sagittal scans, whereas the S-shaped curve before the cardiac sphincter was better imaged in the dorsal plane. In general, the layers of the wall of the digestive tract were seen and the submucosal layer of the esophagus was more visible because of the hyperintensity of the papillae in the T2-weighted image.

The stomach was on the left side of the coelomic cavity, occupying the second and third left quadrants (Figures 1–3). This organ was directly in contact later-

ally with the coelomic membrane, medially with the first part of the duodenum and liver, and ventrally with the left lobe of the liver; dorsally it was separated from the left lung by the coelomic membrane (Figure 7). In T2-weighted images, this organ was easily identified and the volume and intensity of the signal observed in the lumen was inconsistent.

The first part of the duodenum coursed parallel to the caudal border of the liver transversely in the coelomic cavity (Figures 3 and 6) from the second left to the second right quadrants (Figures 1 and 2). Dorsally, in the second right quadrant, the first part of the duodenum received discharge from the gallbladder via a common bile duct that was seen in the anatomic sections but could not be clearly identified on MRI images (Figures 3, 6, and 7). In live turtles, the signal in this part of the small intestine was hyperintense, compared with the liver. The cranial duodenal flexure could be identified when the image was compared with the anatomic sections. In 3 live turtles, it was possible to see points of narrowing of the large intestine (Figure 8) that were interpreted as physiologic, irregular, peristaltic movements. The pancreas, identified in the anatomic sections as a flat structure attached in this region of the coelomic cavity, was difficult to recognize in live turtles because of its isointensity, compared with the liver. In dead specimens, this organ could be identified because of the changes of the liver signal. Dorsally, in the second central quadrant, close to the liver and first part of duodenum, was the spleen, which had an oval to elongated form and yielded a slightly hypointense signal, compared with the liver, in T1-weighted images and a hyperintense signal in T2-weighted images.

The descending colon was better visualized in the dorsal plane scans. It was located craniocaudally on the left side in the third left quadrant (Figures 1 and 3) and was adjoined to the rectum in the fourth central quadrant (Figures 1, 4, and 8).

The liver had 2 lobes that were imaged in the second left and right quadrants (Figures 1 and 2), respectively. In this area, the organ was easily recognized in all planes of the MRI sections (Figures 3 and 6–8). Compared with muscle, the hepatic parenchyma was hyperintense in T1-weighted images and slightly hypointense in T2-weighted images (Figures 7 and 8). The gallbladder had an elliptical form with the major axis oriented almost vertically in the second right quadrant. It was located on the right hepatic lobe and easily recognized in all 3 planes because of its hypointense and hyperintense signals in T1- and T2-weighted images, respectively (Figures 6 and 7). The great left and right hepatic veins coursed transversely in the left and right lobes, respectively, and were visible in both sequences in live turtles and clearly seen in T2-weighted images of dead turtles (Figure 3). Only in 1 turtle could the left hepatic vein be easily recognized in T2-weighted images.

The heart was located ventrally in the coelomic cavity between the first and second central quadrants (Figures 1 and 2) and adjacent to the plastron. The ventricle extended caudally to the hepatic lobes and cranial duodenal flexure (Figure 3). The myocardium

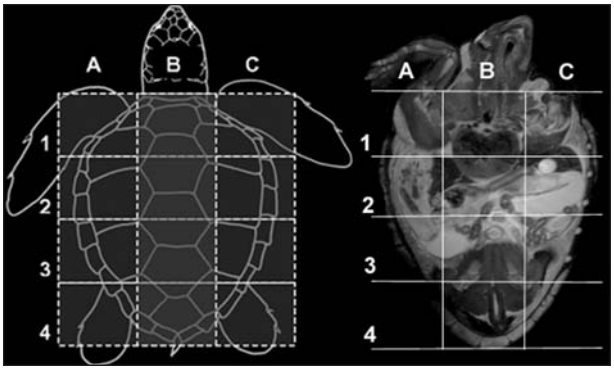

Figure 1—Schematic drawing of the dorsal view of a loggerhead sea turtle, results of corresponding dorsal T2-weighted MRI, and matrix used to describe anatomic structures. 1A = First left quadrant. 1B = First central quadrant. 1C = First right quadrant. 2A = Second left quadrant. 2B = Second central quadrant. 2C = Second right quadrant. 3A = Third left quadrant. 3B = Third central quadrant. 3C = Third right quadrant. 4A = Fourth left quadrant. 4B = Fourth central quadrant. 4C = Fourth right quadrant.

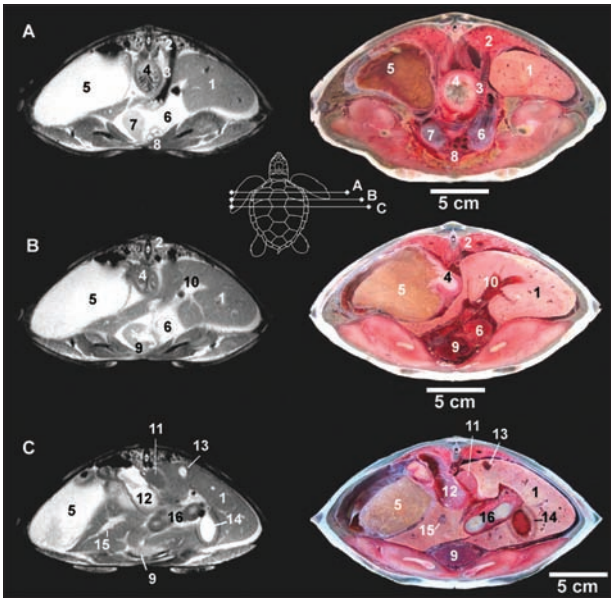

Figure 2—Results of transverse T2-weighted MRI (left column) and corresponding anatomic sections (right column) of a dead loggerhead sea turtle (caudal view) at different levels of the carapace (A, B, and C). Schematic drawing indicates section level. 1 = Liver. 2 = Right lung. 3 = Right bronchus. 4 = Esophagus. 5 = Stomach. 6 = Right atrium. 7 = Left atrium. 8 = Transverse section of large vessels of cardiac base. 9 = Ventricle. 10 = Right hepatic vein. 11 = Spleen. 12 = Large intestine. 13 = Postcava vein. 14 = Gallbladder. 15 = Left hepatic vein. 16 = Duodenum.

had similar signal intensity to pectoral muscles in both sequences, and in the T2-weighted images, the shape of the heart could be identified because of the hyperintense signal of the pericardial fluid in the cardiac sheath (Figure 6). In the transverse MRI section immediately caudal to the junction of the first and second vertebral scutes,[19] it was possible to recognize the transverse section of the great vessels, such as the left and right aorta, pulmonary arteries, and brachiocephalic trunk (Figure 8).

The plastron bones covered most of the ventral surface of the coelomic cavity. However, a large area

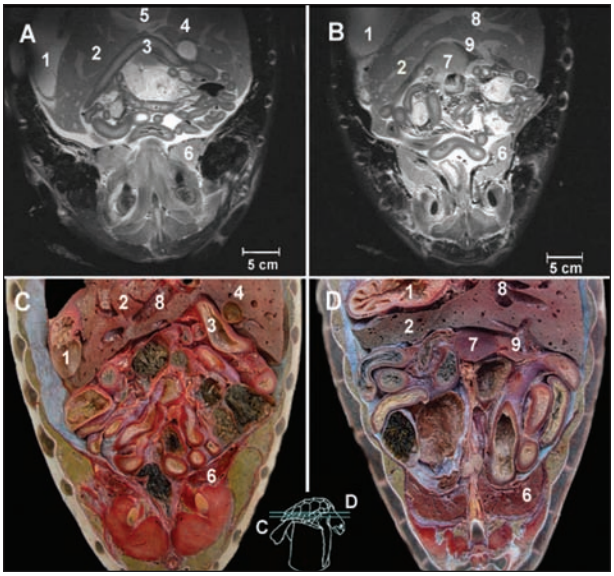

Figure 3—Results of dorsal T2-weighted MRI (A and B) and corresponding anatomic sections (C and D) of a dead loggerhead sea turtle. 1 = Stomach. 2 = Liver. 3 = Duodenum. 4 = Gallbladder. 5 = Ventricle. 6 = Kidney. 7 = Spleen. 8 = Right hepatic vein. 9 = Pancreas.

not protected by bone was identified in the images of the cardiac region of the juvenile specimens (Figure 8) and confirmed on the basis of osteologic preparations (Figure 4).

The junctions between the right and left cranial vena cavae and the left hepatic vein and the caudal vena cava could be imaged in a dorsal scan immediately ventral to the caudal end of the esophagus, revealing a typical flow void signal (Figure 8). The short, thick, right and left renal veins joined and formed the caudal vena cava that coursed cranially, on the right side of the coelomic cavity, toward the heart.

The lungs were located dorsally in the coelomic cavity (Figure 2) and extended approximately three quarters of the carapace length. Because of the great amount of air present, no signal was observed except the discrete thin septa, which resembled a honeycomb structure (Figures 4, 7, and 8). The cranial part of the left and right bronchi was external to the pulmonary parenchyma, and their longitudinal sections were seen in transverse scans of the caudal third of the first central quadrant.

The kidneys were located dorsally in the third left and right quadrants (Figures 1 and 3) and partially in the third central quadrant and were better observed in transverse and sagittal sections. In the latter, the kidneys' shape resembled that of a boomerang with the great curvature inserted in the internal concavity of the carapace. The kidneys were hyperintense in relation to the adjacent muscles in T2-weighted images (Figure 8) and fairly hyperintense in T1-weighted images. Transverse sections of the renal veins and external iliac veins were seen in a transverse scan. Ureters and reproductive structures could not be recognized. In live turtles, the urinary bladder was identified as a result of its fluid content, which was hypointense and hyperintense in T1- and T2-weighted images, respectively. However, the entire contour of the urinary bladder was not well outlined. Signal intensity of some coelomic structures seen in T1- and T2-weighted images was compared with muscle (**Appendix**).

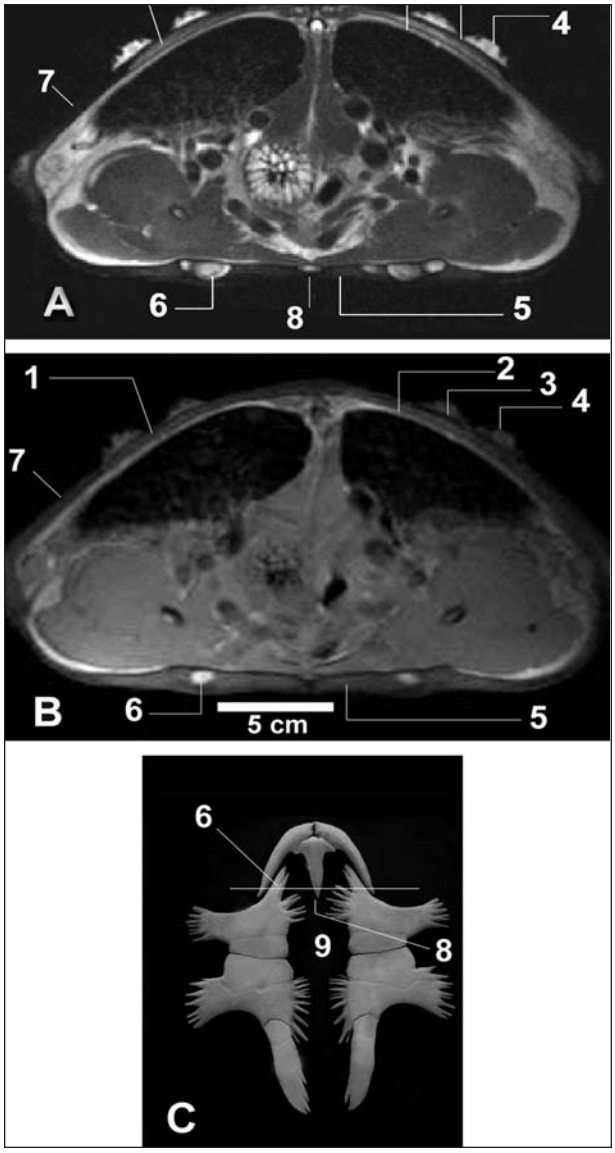

Figure 4—Results of transverse T2- (A) and T1-weighted (B) MRI of a live loggerhead sea turtle and photograph of an osteologic preparation of plastron bones of a loggerhead sea turtle (C). 1 = Flat bone. 2 = Coelomic membrane (coelomic fluid). 3 = Keratinized epidermal layer. 4 = Cirripeds (external parasites). 5 = Connective tissue. 6 = Hyoplastron (plastron bone). 7 = Fontanelles. 8 = Endoplastron (plastron bone). 9 = Cardiac area.

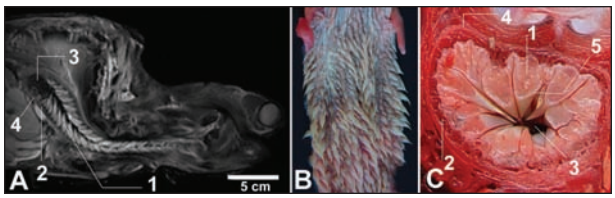

Figure 5—Results of sagittal T2-weighted MRI (A) and gross photographs of the esophagus (B and C) of a loggerhead sea turtle. 1 = Esophageal papillae (projections of submucosa). 2 = Muscular layer. 3 = Lumen (cardiac sphincter). 4 = Serosa. 5 = Keratinized layer.

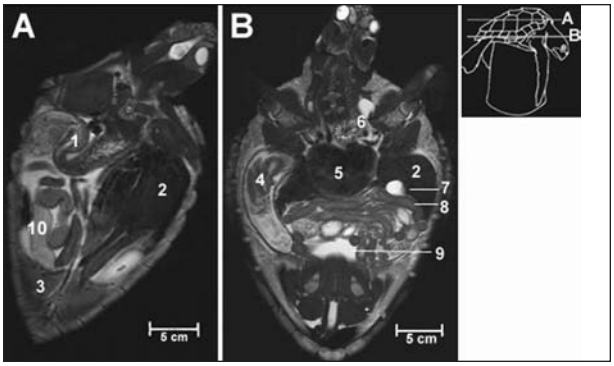

Figure 6—Results of dorsal T2-weighted MRI of the coelomic cavity of a live loggerhead sea turtle at different levels of the carapace (A and B). 1 = Cardiac sphincter. 2 = Liver. 3 = Kidney. 4 = Stomach. 5 = Heart. 6 = Esophagus. 7 = Gallbladder. 8 = Duodenum. 9 = Urinary bladder or coelomic fluid. 10 = Descending colon.

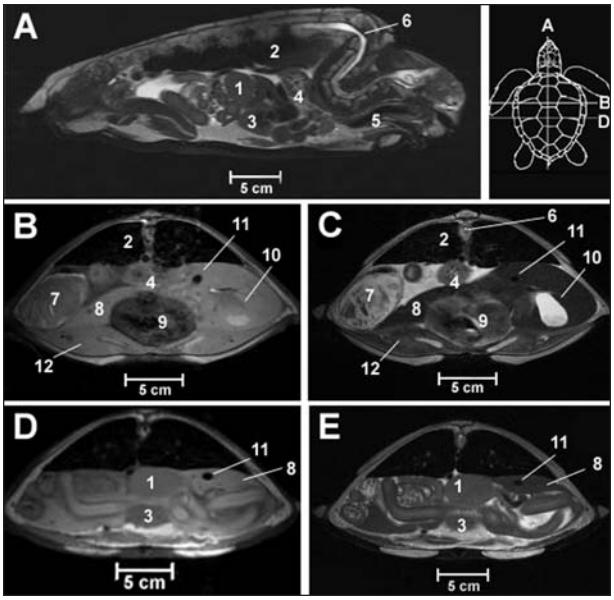

Figure 7—Sagittal T2-weighted image (A) and transverse T1- (left) and T2-weighted (right) images (B–E) from MRI of the coelomic cavity of a live loggerhead sea turtle. 1 = Spleen. 2 = Lung. 3 = Ventricle. 4 = Esophagus. 5 = Trachea. 6 = Spinal cord. 7 = Stomach. 8 = Liver. 9 = Right atrium. 10 = Gallbladder. 11 = Postcava vein. 12 = Pectoral musculature.

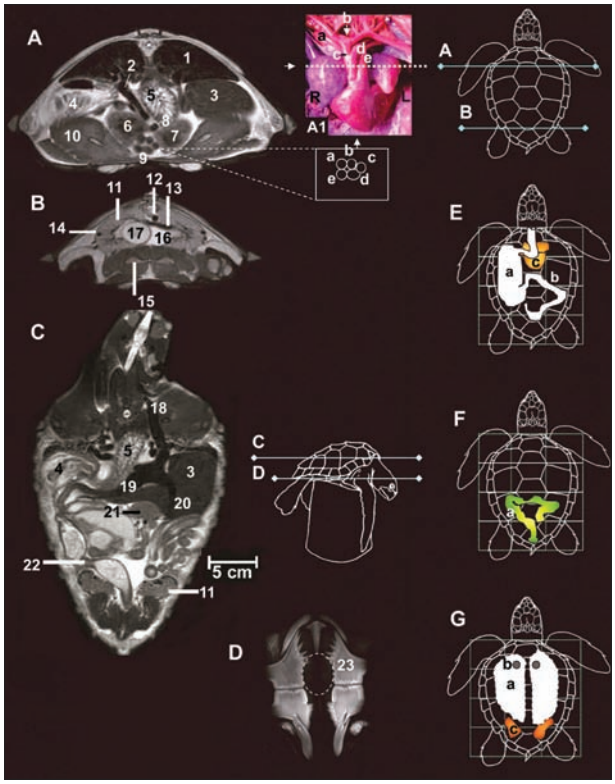

Figure 8—Results of MRI and schematic drawings of topographic anatomic features of a live loggerhead sea turtle. Views A and B—Caudal transverse T2-weighted images. View A1 is a ventral view of an anatomic dissection of the heart injected with latex; notice the right pulmonary artery (a), right aorta (b), brachiocephalic trunk (c), left aorta (d), and the left pulmonary artery (e). Views C and D—Dorsal T2-weighted images; the circular area on View D indicates the cardiac region. View E—Schematic drawing of the stomach (a), duodenum (b), and heart (c). View F—Schematic drawing of the large intestine (a). View G—Schematic drawing of the lungs (a), bronchi (b), and kidneys (c). 1 = Right lung. 2 = Left bronchus. 3 = Liver. 4 = Stomach. 5 = Esophagus. 6 = Left atrium. 7 = Right atrium. 8 = Left aorta. 9 = Transverse section of large vessel of cardiac base. 10 = Pectoral musculature. 11 = Left kidney. 12 = Dorsal aorta. 13 = Renal vein. 14 = External iliac vein. 15 = Pubis and pelvic muscles. 16 = Urinary bladder. 17 = Descending colon. 18 = Right cranial vena cava. 19 = Left hepatic vein. 20 = Caudal vena cava. 21 = Spleen. 22 = Narrowing of large intestine. 23 = Hyoplastron bone.

Discussion

In previous reports[10,12] of MRI in reptilian species, it is stated that most chelonians do not develop major problems during the time required for examination via MRI and may not even require sedation. In the present study, chemical restraint was necessary in addition to the immobilization of the turtle's head and flippers with a large self-adhesive band. Although all live turtles were subjected to the same procedure under similar conditions (ie, similar anesthetic dose, external temperature, body surface humidity, and physical restraint), wide variation in anesthetic effect was observed during the approximately 40 minutes of examination. Immobilization had to be maintained by administering higher doses of anesthesia (up to 3 times the recommended dose), which was still insufficient to prevent slight movements of the flippers and head. Because most studies that used MRI in chelonians were performed on tortoises, we deduced that physical restraint of sea turtles was hampered by the fact that, unlike tortoises, they cannot retract their limbs and head inside the shell. Conversely, the unpredictable response to anesthesia may have been caused by inability of the ketamine-diazepan combination to block reaction to the loud noise made by the magnetic pulses, as has been observed in dogs.[20] In green turtles subjected to MRI examination for detection of internal tumors, a ketamine-medetomidine combination injected 20 minutes before the scan provided adequate sedation.[13] Nevertheless, the unknown individual responses of loggerhead sea turtles to the powerful magnetic field used in MRI (30,000 times greater than the Earth's) need further research, in view of the sea turtle's known ability to orient and navigate by use of electromagnetic fields.[21,22]

Sea turtles may feed on garbage and floating plastic bags, which become hooked on the esophageal digestive

papillae.[23] Macroscopically, the sharp papillae resemble those found on the buccal mucosa of cattle and sheep. By use of the anatomic sections as reference points it was verified that the papillae were formed by projections of the submucosa and had an outer surface covered by a thin keratinized epithelium that was not imaged because of lack of signal. The hyperintense signal observed in the T2-weighted images indicated water in the submucosa, which had a shiny appearance in the anatomic sections. The exact function of these papillae is unknown, but they are presumed to trap food while excess water is expelled prior to swallowing.[19] Magnetic resonance imaging of the esophagus could be important as a complementary method to diagnose esophageal lesions and partial obstructions caused by foreign bodies lodged between or on papillae. The esophageal mucosa is not clearly visualized by use of endoscopy in loggerhead sea turtles because of the large size of the papillae (as long as 2.5 cm), which prevents examination of the underlying mucosa and may obscure small foreign bodies.[24] Lumen narrowing often develops because of the inflammatory reaction and fibrosis at the point where fishhooks are lodged (not only the mucosa but also the submucosa and muscular layers)[25]; therefore, the duration of the healing process in sea turtles is lengthy. By permitting evaluation of the regression of tissue inflammation after removal of the hook is performed surgically or endoscopically, MRI could be recommended as part of a release protocol and would aid in decreasing long stays in the rescue center.

The low-frequency cardiac movements did not create artifacts that compromised image interpretation. Although most internal viscera are protected by rigid tissue (dermal bones), the cardiac region was surprisingly unprotected as seen by use of MRI. The information obtained via MRI concurred with observations made by the authors on osteologic preparations of juvenile turtles. We believe that these findings have not been reported because previous studies lacked evaluation of the cross-sectional relationship between the skeleton and the internal viscera. The scant ossification of the medial edges of the hyoplastron bones in juvenile turtles could make them more susceptible to compression in trawling nets.

Although better images were obtained by use of T2-weighted images, it is clinically important to perform the 2 sequence types because T1-weighted images could reveal changes in the water or fat concentrations in organs, indicating the possibility of infiltrative inflammatory processes, edema, liver fat degeneration, splenitis, or hydronephrosis. Likewise, T1-weighted images could be useful in sea turtle rehabilitation for detecting crude oil ingestion, a frequent finding in dead turtles.[25]

Topographic anatomic features and their correlation with MRI are well documented in various mammalian species.[26-30] Although we could not find reports of studies that used methodology comparable to that of the present study, comparison of the internal organs of turtles with those of dogs scanned at 1 Tesla unit revealed the same difficulties in visualizing the pancreas caused by the small amount of contrast with the intestine.[30] The spleen of loggerhead sea turtles had the best contrast in T2-weighted images, compared with dogs, in which T1-weighted sequences provided the best contrast. The alimentary canal of dogs is best evaluated by use of moderated T1-weighted images because they provide good contrast between the intestine wall and the surrounding fatty tissue.[30] In the present study, T2-weighted images provided the best visualization of the alimentary canal. This difference could be related to the nutritional status of the free-ranging turtles used in this study, which did not have the large fat deposits in the mesentery that typically occur in domestic and captive animals.

In dogs, the kidneys are best delineated by T1-weighted sequences, which provide good contrast between the medulla and the cortex. Because turtles do not have 2 distinct renal layers, the layers observed in dogs are not seen in loggerhead sea turtles.[30] Unlike dogs, the turtle kidneys were best recognized in T2-weighted images and had a heterogeneous parenchyma with high blood supply.

The morphologic characteristics of chelonians cause difficulties in applying conventional techniques for location and examination of the coelomic organs. The carapace has 2 main layers, the inner bony dermal layer and the outer scaly epidermal layer.[31] Differentiation of these layers observed in the transverse MRI sections was attributable to the presence or absence of osseous structures and connective tissues at specific points of the carapace. The thin layer formed by compact bone and the outer keratinized epidermal layer account for the lower signal observed along the external periosteal surface of the bone. These layers could be identified only in those turtles with cirripeds encrusted in their shell because cirripeds act as hyperintense landmarks that permit identification of the thickness of the hypointense outer layer. Cancellous bone found in the flat bones of the carapace and plastron had a hyperintense signal, compared with the cortical bone; this is attributable to the presence of bone marrow, as in dogs and cats.[32] The fontanelles were quite wide in all turtles studied and, therefore, provided a hypointense signal in the T2-weighted image.

Although the gross anatomic features of the loggerhead sea turtles were similar to other sea turtles,[19] differences in the signal intensity of some tissues were observed. In T2-weighted images of spur-thighed tortoises and Aldabran tortoises, blood vessels had a hyperintense signal and the liver and heart were more hyperintense than the pectoral musculature.[10] Also, in green turtles, the branching pulmonary vasculature was easily seen in the dorsal plane because of the contrast between its hyperintense signal and the hypointensity of the pulmonary parenchyma.[13] In healthy loggerhead sea turtles, the blood and, consequently, vascular structures had a typical void signal. Likewise, the signal intensity of the myocardium, compared with the skeletal muscle, in T2-weighted images was isointense in loggerhead sea turtles, whereas it was slightly hyperintense in green turtles.[13] The same appearance of the blood vessels and liver observed in those chelonian species was seen in dead loggerhead sea turtles in the present study. This change in signal intensity, observed mainly in the blood vessels and high blood supply structures of dead turtles, was also observed in MRI of dead turtles and was related to the absence of blood flow.[f] Caution is therefore recommended for future descriptions of MRI studies because

dead turtles yield different signals than live turtles and should not be included indiscriminately in such studies.

Detailed images of small chelonians may be obtained when the whole body is scanned. In large chelonians such as sea turtles, the size of field of view (50 × 50 cm) and the gantry limits the single-scan whole-body examination. In this study, most of the turtles were juvenile, so they were placed into the gantry sideways to image the whole body in a single examination. However, a dead subadult sea turtle scan requires 2 steps, which requires examination time of 95 minutes and makes it unsuitable for a live turtle because of the risks involved with prolonged anesthesia.

a. Excelart, Medical Systems, Toshiba Co, Tokyo, Japan.
b. Imalgene 1000, Merial, Saint Priest, France.
c. Diazepam prodes injectable, Almirall Prodesfarma, Barcelona, Spain.
d. Digital still camera, Sony DSC-F707, Sony Corp, Tokyo, Japan.
e. Photoshop, version 5.5, Adobe Systems Inc, San Jose, Calif.
f. Snellman M. *Magnetic resonance imaging in canine spontaneous neurological disorders: an evaluation of equipment and methods*. Academic dissertation, Section of Veterinary Diagnostic Imaging, Department of Clinical Veterinary Sciences, Faculty of Veterinary Medicine, University of Helsinki, Helsinki, Finland, 2000.

Appendix—T1- and T2-weighted MRI signals of coelomic structures of loggerhead sea turtles, compared with signals from muscle.

Organ or structure	T1-weighted	T2-weighted
Myocardium	Isointense	Isointense
Liver	Hyperintense	Hypointense
Spleen	Isointense	Hyperintense
Kidneys	Hyperintense	Hyperintense
Fat tissue	Hyperintense	Hyperintense
Compact bone	Hypointense	Hypointense
Cancellous bone (carapace and plastron)	Hyperintense	Hyperintense

References

1. Damadian RV. Tumor detection by nuclear magnetic resonance. *Science* 1971;171:1151–1553.
2. Schreiber WG, Teichmann EM, Schiffer I, et al. Lack of mutagenic and co-mutagenic effects of magnetic fields during magnetic resonance imaging. *J Magn Reson Imaging* 2001;14:779–788.
3. Dennis R. Estudio por imágenes de resonancia magnética, perspectiva general de su uso actual en medicina veterinaria. *Vet Int* 1995;2:52–61.
4. Tucker RL, Gavin PR. Brain imaging. *Vet Clin North Am Small Anim Pract* 1996;26:735–758.
5. Nicholas Joseph Jr RT. Protection and safety from energies used in: x-ray, CT, nuclear medicine and PET, and MRI part VI MRI safety for health care personnel. Radiographic Imaging CEU Source LLC Web site. Available at: www.radiographicceu.com/article12.html. Accessed Feb 6, 2006.
6. Walzer C, Url A, Robert N, et al. Idiopathic acute onset myelopathy in cheetah (*Acinonyx Jubatus*) cubs. *J Zoo Wildl Med* 2002;34:36–46.
7. Jandial R, Greenberg MS, Aryan HE et al. Lumbar diskectomy in a human-habituated western lowland gorilla. *Internet J Neurosurg* [serial online]. 2005;2:1–11. Available at: www.ispub.com/ostia/index.php?xmlFilePath=journals/ijns/front.xml. Accessed Jul 25, 2005.
8. Thornton SJ, Hochachka PW, Crocker DE, et al. Stroke volume and cardiac output in juvenile elephant seals during forced dives. *J Exp Biol* 2005,208:3637–3643.
9. Rübel A, Kuoni W, Augustiny N. Emerging techniques: CT scan and MRI in reptile medicine. *Semin Avian Exot Pet Med* 1994;3:156–160.
10. Wilkinson R, Hernandez-Divers S, Lafortune M, et al. Diagnostic imaging. In: McArthur S, Wilkinson R, Jean M, eds. *Medicine and surgery of tortoises and turtles*. Victoria, Australia: Blackwell Publishing Ltd, 2004;187–238.
11. Raiti P, Haramati N. Magnetic resonance imaging and computerized tomography of a gravid leopard tortoise (*Geochelone pardalis pardalis*) with metabolic bone disease. *J Zoo Wildl Med* 1997;28:189–197.
12. Straub J, Jurina K. Magnetic resonance imaging in chelonians. *Semin Avian Exot Pet Med* 2001;10:181–186.
13. Croft LA, Graham JP, Schaf SA, et al. Evaluation of magnetic resonance imaging for detection of internal tumors in green turtles with cutaneous fibropapillomatosis. *J Am Vet Med Assoc* 2004;225:1428–1435.
14. Convention on international trade in endangered species of wild fauna and flora Web site. Appendices I, II and III. Availaible at: www.cites.org/eng/app/appendices.shtml Accessed Apr 6, 2005.
15. Aguilar R, Pastor X. Impact of Spanish swordfish longline fisheries on the loggerhead sea turtle, *Caretta caretta*, population in the western Mediterranean, in *Proceedings*. 12th Annu Symp Sea Turtle Biol Conserv 1992;FSC 361, 1–6.
16. Pont SG, Alegre FN. Work of the Foundation for the Conservation and Recovery of Marine Life. *Marine Turtle Newsletter* 2000;87:5–7.
17. Dodd CK Jr. *Synopsis of the biological data on the loggerhead sea turtle* Caretta caretta *(Linnaeus 1758)*. *US Fish and Wildlife Service biological report 88(14)*. Washington, DC: US Fish and Wildlife Service, 1988;35–82.
18. Bolten A. Techniques for measuring sea turtles. In: Eckert KL, Bjorndal KA, Abreu-Grobois FA, et al, eds. *Research and management techniques for the conservation of sea turtles*. *IUCN/SSC marine specialist group publication No. 4*. Washington, DC: IUCN Species Survival Commission, 1999;110–115.
19. Wyneken J. *The anatomy of sea turtles. US Department of Commerce NOAA Technical Memorandum NMFS-SEFSC-470*. Washington, DC: US Department of Commerce, 2001.
20. Shore A. Magnetic resonance imaging. *Vet Clin North Am Small Anim Pract* 1993;23:437–459.
21. Irwin WP, Lohmann KJ. Magnet-induced disorientation in hatchling loggerhead sea turtles. *J Exp Biol* 2003;206:497–501.
22. Avens L, Lohmann KJ. Navigation and seasonal migratory orientation in juvenile sea turtles. *J Exp Biol* 2004;207:1771–1778.
23. McArthur S. Problem-solving approach to conditions of marine turtles. In: McArthur S, Wilkinson R, Jean M, eds. *Medicine and surgery of tortoises and turtles*. Victoria, Australia: Blackwell Publishing Ltd, 2004;301–307.
24. Pressler BM, Goodman RA, Harms CA, et al. Endoscopic evaluation of the esophagus and stomach in three loggerhead sea turtles (*Caretta caretta*) and a malaysian giant turtle (*Orlitia borneensis*). *J Zoo Wildl Med* 2003;34:88–92.
25. Orós J, Torrent A, Calabuig P, et al. Diseases and causes of mortality among sea turtles stranded in the Canary Islands, Spain (1998–2001). *Dis Aquat Organ* 2005;63:13–24.
26. Colaço B, Ferreira D, Gonzalo-Ordén M, et al. The use of magnetic resonance imaging in the study of canine brain anatomy. *Rev Port Cienc Vet* 2003;548:159–165.
27. Marino L, Sudheimer K, Pabst DA, et al. Magnetic resonance images of the brain of a dwarf sperm whale (*Kogia simus*). *J Anat* 2003;203:57–76.
28. Glyde M, Doyle R, McAllister H, et al. Magnetic resonance imaging in the diagnosis and surgical management of sacral osteochondrosis in a mastiff dog. *Vet Rec* 2004;155:83–86.
29. Murray R, Tim M. Use of magnetic resonance imaging in lameness diagnosis in the horse. *In Pract* 2005;27:138–146.
30. Assheuer J, Sager M. *MRI and CT atlas of the dog*. Berlin: Blackwell Science Ltd, 1997;347–403.
31. Burke AC. The development and evolution of the turtle body plan: inferring intrinsic aspects of the evolutionary process from experimental embryology. *Am Zool* 1991;31:616–627.
32. Armbrust LJ, Hoskinson JJ, Biller D, et al. Low-field magnetic resonance imaging of bone marrow in the lumbar spine, pelvis and femur in the adult dog. *Vet Radiol Ultrasound* 2004;5:393–401.